Joint Power-Rate-Slot Resource Allocation in Energy Harvesting-Powered Wireless Body Area Networks

Zhiqiang Liu, *Student Member, IEEE*, Bin Liu, *Member, IEEE*, and Chang Wen Chen, *Fellow, IEEE*

Abstract—Wireless body area network (WBAN) has become a promising network for continuous health monitoring of various diseases. The limited energy of sensors in WBAN cannot support the long term work with the high requirements of Quality of Service (QoS) for health applications. Energy harvesting (EH)-powered WBAN, which can provide uninterrupted work, has attracted more attention from both macadamia and industry. However, the time-varying and heterogeneous EH states of different sensors become an important factor when designing the resource allocation schemes in EH-powered WBAN. In this paper, we propose a novel two-phase resource allocation scheme, which optimizes the allocation of transmission power, source rate and slots to improve the QoS performance of EH-powered WBAN. In the first phase, we analysis the relationship between the QoS performance and the source rate for satisfying the Energy Neutral Operation (ENO), and then a joint Power-Rate Control Scheme (PRCS) is proposed to optimize the source rate and transmission power for ensuring the long-term QoS performance based on the statistical properties of EH. Moreover, we design a QoS Aware Slot Allocation Scheme (QASAS) to dynamically adjust the time slot allocation to cope with the time-varying and heterogeneous EH states for obtaining better short-term QoS performance in the second phase. Finally, numerical simulation results demonstrate that the proposed joint the Power-Rate-Slot resource allocation scheme of EH-powered WBAN can effectively exploit the time-varying EH to improve both long-term and short-term QoS performance.

Index Terms—energy harvesting, resource allocation, wireless body area network (WBAN).

I. INTRODUCTION

With the rapid development of sensor and wireless communication technologies, wireless body area network (WBAN) can replace complex and wired healthcare applications to continuously monitor the body's vital signals and provide real-time feedback to the user and doctors without causing any discomfort and interrupting their daily lifestyle [1–3]. WBAN typically consists of several low-power, miniaturized and lightweight on-body or implanted sensor nodes to monitor physiological parameters, and then these collected physiological data are further transmitted to remote medical servers by one energy-efficient hub (Mobile phone or PDA) for various medical and healthcare applications [4]. Generally, most of

Zhiqiang Liu is with the Key Laboratory of Electromagnetic Space Information, Chinese Academy of Sciences, Department of Electrical Engineering and Information Science, University of Science and Technology of China, Hefei 230027, China (e-mail: lzhq28@mail.ustc.edu.cn).

Bin Liu is with the Key Laboratory of Electromagnetic Space Information, Chinese Academy of Sciences, School of Information and Technology, University of Science and Technology of China, Hefei 230027, China (e-mail: flowice@ustc.edu.cn).

Chang Wen Chen is with Department of Computer Science and Engineering, University at Buffalo, State University of New York, New York 002837, USA (e-mail: chencw@buffalo.edu).

these applications are related to the chronic diseases, which need to continuously monitor the body's vital signals without interrupting user's daily lifestyle. In addition, for carrying out an effective diagnosis, the Quality of Service (QoS) should be guaranteed in terms of packet loss, delay and so on [5].

However, the limited battery capacity, constrained by the size and weight of sensors nodes, cannot support the long term operation without interruption. Besides, replacing battery or taking off sensors to charge power is not always practical especially for some implanted sensors, which also causes the interruption of the health monitoring system [6, 7]. Although the classical energy saving technologies make efforts to explore different energy efficient schemes in aspects of MAC protocol design, power control schemes and cross-layer resource scheduling strategies to prolong the system lifetime [4, 8, 9], the ultimate goal 'uninterrupted work' cannot be ensured. Fortunately, Energy Harvesting (EH) technology, which can collect energy from various sources around human body, has recently been considered as a promising solution to overcome the bottleneck of energy limited WBANs [10]. For instance, EH-powered sensors can scavenge energy from a variety of ambient sources (e.g., light, heat, electromagnetic radiation) or the body itself (e.g., locomotion, breathing, heartbeat, lactate), and then convert it to usable electric energy for providing continuous power [11]. Thus, EH-powered WBANs have the potential ability to achieve infinite lifetime and perpetual operation, which is called Energy Neutral Operation (ENO) [12]. Furthermore, sensors can also combine several types of EH sources for acquiring more energy to support more strict QoS requirements [6]. Therefore, researchers have paid more and more attentions on how to keep in ENO state with considering the QoS performance in EH-powered WBAN.

In the literature, most of researchers investigated the statistical characteristics of the energy harvesting in the resource allocation schemes to support the long-term QoS performance [13][14][6]. However, sensors in different positions on the body may have different types of EH and the energy collection rates are heterogeneous. Meanwhile, harvesters with energy sources from the human body have time-varying states caused by the dynamic body movement status, and then the collected available energy is time-variant and different for each node to transmit data packets. Therefore, the time-varying EH states can be exploited to dynamically allocate the resource for improving the short-term QoS performance. This phenomenon will lead to a significant result: the time-varying and heterogeneous EH states become a significant factor to design the effective resource allocation scheme for improving both the long-term QoS performance and the short-term QoS performance.

A. Related works

Compared with EH-powered wireless sensor networks (WSNs), the human body contains more bio-energy sources besides the ambient source for various kinds of energy harvesters in WBANs [14]. Generally, these bio-energy sources can be classified into biochemical and biomechanical energy sources. The biochemical energy sources convert electrochemical reactions to electricity for implanted body sensors, while the harvesters can scavenge energy from the voluntary and involuntary actions of the human body as biomechanical energy sources [11]. The scavenged energy can be converted to electric potential by appropriated harvesters, and then stored into a rechargeable battery or a super-capacitor for powering up wireless body sensors [15]. The energy harvesting efficiency can be improved to harvest more energy through the elaborate hardware circuit design [16][17]. Therefore, the available power density by harvesting energy from human body gradually reaches μW range, which is able to run low-power-consuming wireless devices, such as Bluetooth4.0 [18], MicaZ [19], MultiMode [20] and so on. However, the harvesting process of human body sensors is unstable and time-varying due to the dynamic body movement status [10]. Thus, the time-varying EH states should be taken full consideration into the resource allocation schemes.

In the literature, some researches have focused on the resource allocation schemes for EH-powered WBANs. Generally, these resource allocation schemes can be divided into two categories in terms of the priori knowledge of the channel state, data state and energy state for the transmitter: the offline schemes [21–26] and the online schemes [6, 13, 14, 27–30]. For the offline schemes, it is assumed that the transmitter has the perfect priori knowledge of the channel state, data state and the energy state when it allocates resources. In [24], the short-term throughput and the transmission completion time were regarded as the objective function to obtain the optimum power allocation with a deadline constraint and finite energy storage capacity, while energy arrivals were assumed as a priori known. Shan et al., [23] proposed a general framework to transform a continuous-rate model into practical discrete transmission rates with keeping the optimality, and the per-application quality-of-service (QoS) could be guaranteed by the optimal rate scheduling algorithm for an EH enabled transmitter, assuming that the information regarding packets and harvesting is known in advance. Varan et al., [22] considered the throughput maximization problem with finite energy and data storage constraints, and new notions of water pumps and overflow bins were added to the directional water-filling for solving the energy scheduling problem. In addition, the weighted sum of the outage probabilities was the objective function to be minimized in the power control policy, while the harvested energy was known as a priori to the scheduler, and a near-optimal offline scheme was designed with only high signal-to-noise ratios due to the non-convex objective function [25, 26]. The above offline resource allocation schemes commonly construct the convex optimization problems and analytical solutions to obtain the optimal resource allocation results with perfect non-causal and priori knowledge. Thus,

offline schemes can only serve as a benchmark of the resource allocation schemes, or the EH states are predictable for some stable energy sources.

Compared with the offline schemes, only the causal information and statistical knowledge of energy states, data states and channel states can be utilized in the online schemes to manage the data packets and the collected energy. Ozel et al., [13] maximized the number of bits sent by a deadline given only the distributions of the energy arrivals and channel fade levels. Leng and Yener [14] maximized the long-term expected throughput under the energy constraints, and the close-form expression of optimal transmission power was obtained by formulating the Largrangian and solving the KKT conditions. However, the long-term throughput maximization problem only allocates the resources from the statistical characteristics of EH states. The time-varying EH states, which have a great effect on the transmissions of packets, are not mentioned. Liu et al., [30] modeled the transmission power and time allocation optimization problem as a Markov decision process (MDP) to provide a sustainable and high quality service for EH-powered WBAN. However, MDP based resource allocation schemes have the high complexity for wireless devices with limited computational capabilities in WBANs, and they are highly dependent on the accuracy models of channel fading level, energy arrivals and data arrivals, which are hardly obtained in practice. To achieve the best possible QoS performance, the authors of [6] proposed a joint power-QoS control scheme for making optimal use of harvested energy to efficiently transmit the respective data packets of only one sensor in WBAN. However, the channel fading was not considered in the scheme, which could not deal with the dynamic link characteristics in WBANs. In addition, the time-varying and heterogeneous EH states of different body sensors were not fully considered.

B. Contributions

In this paper, we take the time-varying and heterogeneous EH states into consideration. And then we develop an efficient resource allocation scheme for EH-powered WBANs to support both the long-term and short-term QoS requirements. The important contributions of this paper are expressed as three aspects:

1) As far as we know, this work is the first to combine the transmission power, source rate and time slots to effectively allocate the resources under dynamic link characteristics of heterogeneous body sensors. The time-varying EH states are regarded as a important factor to reallocate the resources to cope with the variation of the harvesting available energy. Hence, the harvested energy can be efficiently utilized to improve both the long-term and short-term QoS performances.

2) For supporting the long-term QoS performance of body sensors, we design a power-rate control scheme to optimize the transmission power and the source rates for different body sensors, subject to the long-term QoS requirements under the Energy Neutral Operation (ENO). The statistical knowledge of energy harvesting and channel fading are investigated to measure the

QoS performance with the allocated resources. Then, an optimal numerical solution is successfully obtained through the transformation of the non-convex problem.

3) To further improve the short-term QoS performance and the resource utilization, the time-varying and heterogeneous EH states are carefully studied, which cause the fluctuation of the available energy and the data queues. Thus, the energy states and the queue states are evaluated and adopted to predict the states of each sensors. Finally, we propose a QoS aware slot allocation scheme to dynamically adjust the time slot allocation based on the states of each sensors for better transmitting data packets with the harvesting available energy.

The remainder of this paper is organized as follows. In Section II, the system model is presented. In Section III, the relationship between the source rate and the QoS peformance is described in details, and a join power and source rate optimization allocation problem is formulated and solved. In Section IV, the sensor states are evaluated based on the energy state and queue buffer state, and a short-term QoS aware slot allocation scheme is provided in details. In Section V, the numerical results are discussed and analyzed. Finally, Section VI concludes the paper.

II. SYSTEM MODEL

In this section, we give the details of node's architecture and WBAN topology in EH-based WBAN. Then, the energy harvesting model is introduced. Finally, the energy consumption model is correspondingly obtained with the dynamic link characteristics.

A. Node's Architecture and WBAN Topology

We consider a classical WBAN which consists of one hub and N EH-powered wireless sensor nodes. Suppose that the hub (such as a PDA and a mobile phone) has sufficient resources to implement some resource allocation scheme with high computation complexity, and the wireless sensor nodes placed in different positions of the body have limited processing and storage resources with energy harvesters. The set of body sensor nodes is expressed as $\mathcal{C}_{node} = \{1, 2, \cdots, N\}$. As recommended by IEEE 802.15.6 [31], the body sensor nodes collect the vital signals and communicate directly with the hub, and a star topology is adopted with considering the constrained resources of sensor nodes. In addition, a scheduled access mechanism in beacon mode with superframe boundaries is adopted to access the channel without collisions, idle listening and overhearing of sensor nodes for saving scarce energy. One superframe is formed by one beacon and M slots, and the set of slots are expressed as $\mathcal{C}_{slot} = \{1, 2, ..., M\}$. In the beacon of superframe, the hub broadcast the beacon packets to configure the transmission rates, source rates and dedicate time slots for each node. And the node only turns active in its dedicate time slots to transmit data signals, and turn sleep in other slots for saving energy. In each node, the vital signals are collected and packetized in the data queue, which will be transmitted to the hub with the First-In-First-Out (FIFO) queue strategy and the retransmission strategy [32]. Thus, the packet losses only

occur in two situations: data queue overflow and the delay over the preset threshold.

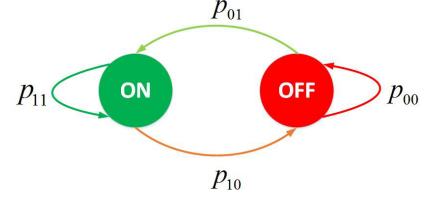### B. Energy Harvesting Model

Fig. 1: Discrete Two-state Markov Chain of the EH process

Due to the different positions and functions of different sensor nodes, the adopted energy harvesters may collect energy from different energy sources. For instance, the sensor node on the foot can utilize the piezoelectric transducer to harvest energy from the body motion [33], and the sensor node for capturing the electrocardiograph (ECG) signal may use a thermoelectric generator to harvest from the body temperature [34]. Therefore, the EH states of different nodes are heterogeneous. In this paper, the harvested energy is stored in a rechargeable battery or a super-capacitor, then used to power the body sensor node [11]. The EH process of each node can be model as a correlated discrete-time Markov chain with two state: the active state (ON) and the inactive state (OFF) [6, 35]. In the ON state, it means the intensity of the motion is conductive to generate the energy by the energy harvester. In the OFF state, the energy harvester does not collect any energy due to the low motion intensity. In addition, the coherence time of the EH process is set to $t_{cor} = k \cdot t_{slot}$, where t_{slot} is the time length of one time slot in the superframe. We assume that the energy acquisition rate in the ON state follows an uniform distribution in range of $[EH_{min}, EH_{max}]$, which is based on intensity of body movement. In addition, the energy acquisition rate in the ON state are different for different sensor nodes. The Markov chain of EH process is shown in Fig. 1. p_{01} means the transition probability from OFF state to ON state, while p_{10} represents the transition probability from ON state to OFF state. The probability of keeping ON state and OFF state are regarded as $p_{11} = 1-p_{10}$ and $p_{00} = 1-p_{01}$, respectively. And the steady probabilities of ON state and OFF state are expressed as follows,

$$\mu_{on} = \frac{p_{01}}{p_{01} + p_{10}} \qquad (1)$$

$$\mu_{off} = \frac{p_{10}}{p_{01} + p_{10}} \qquad (2)$$

C. Energy Consumption Model

In body sensor nodes, most of the energy is consumed to transmit data packets and recieve ACK packets, while the energy consumption of the processing and beacon listening can be ignored [36]. Generally, the transmission energy consumption consists of two parts: the transmit amplifier energy consumption E_{tx} and the circuitry energy consumption E_{ct}

[32, 37]. Thus, the energy model of transmitting packets can be expressed as follows,

$$E_{tran} = (1 + \alpha) E_{tx} + E_{ct} \tag{3}$$

Compared with the energy consumption of transmitting packets, the energy model of receiving packets only contains the circuitry energy consumption E_{ct}.

$$E_{rec} = E_{ct} \tag{4}$$

where α means the power amplifier inefficiency factor, $E_{tx} = P_{tx}t$ and $E_{ct} = P_{ct}t$. P_{tx} represents the transmission power of the transmitter, and P_{ct} is the circuitry power, which is a constant depending on the specific transmitter [38].

To improve the QoS requirements, the transmission power should be dynamically adjusted to cope with the time-varying link quality. Thus, the path loss model of wireless links become a important factor for the energy consumption. In this paper, the path loss model $PL(d)$ for both Light-Of-Sight (LOS) and None-Light-Of-Sight (NLOS) scenarios follows the log normal distribution as recommended by IEEE 802.15.6 [31].

$$PL(d) = PL_{d_0} + 10n\log_{10}\left(\frac{d}{d_0}\right) + X_\sigma \tag{5}$$

where PL_{d_0} is the path loss at the referent distance d_0, and n represents the path-loss exponent. The shadowing X_σ follows the normal distribution $\mathcal{N}\left(\mu_s, \sigma_s^2\right)$, and the statistic characteristics are related to the human postures and the environments [39][40].

III. LONG-TERM POWER-RATE CONTROL SCHEME

In this section, the throughput maximization problem is designed to maximize total throughput with the time-varying EH states, subject to the long-term QoS constraints. Then, the optimal numerical solution is given to solve the optimization problem efficiency through the convex transformation. Finally, the source rate is configured based on the optimal throughput results, with considering the effective diagnosis and energy saving.

A. Throughput Maximization Problem

The QoS requirements should be guaranteed for the effective diagnostic, when designing the resource allocation scheme. Considering the dynamic link characteristics, the exact link quality cannot be known as a priori in the online scheme. In this paper, the average PLR performance is regarded as the main long-term QoS constraint. With the statistic knowledge of the path loss model, the average PLR can be derived through the following equations. Firstly, the PLR can be expressed as the function of the bit Signal to Noise Ratio (bit SNR),

$$PLR(\gamma) = 1 - (1 - P_{b,B}(\gamma))^L \tag{6}$$

where bit SNR can be calculated as $\gamma = 10^{\frac{P_{tx,dB} - PL(d) - P_N}{10}} \frac{B}{R}$. L is the length of a packet in bits. $P_{tx,dB}$ is the transmission power in dB. P_N is the power of noise. B represents the system bandwidth. $P_{b,B}$ indicates the equivalent bit error rate based on the modulation and the channel coding [41].

Then, the average PLR is the mean value over the range of bit SNR with its probability density function. It can be calculated as the following equation.

$$\overline{PLR} = \int_0^{+\infty} PLR(\gamma)P(\gamma|\mu_{\gamma_{dB}}, \sigma_{\gamma_{dB}})d\gamma \tag{7}$$

where $P(\gamma|\mu_{\gamma_{dB}}, \sigma_{\gamma_{dB}})$ represents the probability density function of bit SNR γ, and it follows a log-normal distribution as the shadowing X_σ. $\mu_{\gamma_{dB}}$ and $\sigma_{\gamma_{dB}}$ are the mean and the standard deviation of γ in dB, respectively.

Finally, the long-term QoS constraint can be depicted that the average PLR should be less than the preset threshold as follows,

$$\overline{PLR} < PLR_{th} \tag{8}$$

where PLR_{th} is the preset threshold of the packet loss rate.

As we all know, larger transmission power can obtain better QoS performance, however, the achievable throughput is lower due to the larger energy cost per bit. Thus, not only the long-term PLR performance but also the achievable throughput should be taken into consideration. Besides, the energy acquisition rate of the energy harvester decides how much energy can be collected to transmit data packets. Considering the time-varying and heterogeneous EH states, the average collect energy is time-variation. Therefore, the achievable throughput is constrained by both the QoS performance and the EH states. In this paper, we optimize the allocation of the transmission power to maximize the throughput, subject to the long-term PLR performance and the EH states. The throughput maximization problem can be constructed as follows,

$$\textbf{P1:} \quad \max_{(P_{tx,i}, v_i)} \sum_{i=1}^{i \in \mathcal{N}} v_i, \tag{9a}$$

$$s.t. \quad 0 \le \frac{v_i}{1 - PLR_{i,th}}, \tag{9b}$$

$$\frac{v_i}{1 - PLR_{i,th}} \le \frac{\mu_{on} \cdot R \cdot \overline{EH_i}}{[(1 + \alpha) P_{tx,i} + P_{ct,i}]}, \tag{9c}$$

$$\overline{PLR_i} \le PLR_{i,th}, \tag{9d}$$

$$P_{tx,\min} \le P_{tx,i} \le P_{tx,\max}, \tag{9e}$$

where v_i represents the throughput for node i, and $PLR_{i,th}$ is the threshold of the packet loss rate for node i. $\overline{EH_i} = (EH_{i,\max} + EH_{i,\min})/2$ is the mean of the energy harvesting rate for node i. $\overline{PLR_i}$ represents the average packet loss rate with the allocation transmission power P_i. $P_{tx,min}$ and $P_{tx,max}$ are the minimum value and the maximum value of the transmission power for the transmitter, and we assume all the nodes have the same type transmitter for the sake of simplicity.

With respect to **P1**, the objective function (9a) is to maximize the total throughput under the long-term QoS constraints. The constraint (9b) means the throughput should be not less than zero. In addition, the average collected energy by the energy harvester can be evaluated by exploring the statistical characterization of the EH states, and then the equivalent throughput with considering PLR has a upper boundary which just cost the average collected energy as expressed in constraint (9c). In constraint (9d), the allocated transmission power should guarantee the long-term average PLR perfor-

mance. Equation (9e) means the allocated transmission power should be in the range of $[P_{tx,min}, P_{tx,max}]$.

B. Optimal Numerical Solution

The above optimization problem **P1** is a nonlinear and non-convex problem, and it is difficult to be solved. Fortunately, we find that the optimization problem **P1** is quit similar to the form of the Geometric Program (GP), which can be solved efficiently and reliably [42]. Thus, we try to transform the problem **P1** into the form of the Geometric Program (GP).

Obviously, the objective function (9a) is a posynomial function. And all constraints, expect (9c) and (9d), can be easily converted to the form of a posynomial less than or equal to one. Fortunately, both constraints (9c) and (9d) can be successfully transformed into the form of posynomial inequalities through the following methods.

Firstly, the PLR constraint (9d) has not an analytical expression, however we have proved that the average PLR constraint is the monotone function of bit SNR in [9]. Therefore, the PLR constraint can be equivalent to the constraint of the mean of bit SNR as follows,

$$\mu_{\gamma_{dB}} \geq \mu_{th} \qquad (10)$$

where μ_{th} just satisfies the equation $\overline{PLR(\mu_{th})} = PLR_{th}$. And $\mu_{\gamma_{dB}} = E\left[10\log_{10}\left(\frac{B}{R}\right) + P_{tx,dB} - PL(d) - P_N\right]$. Then, the equivalent PLR constraint can be expressed as follows,

$$P_{tx}R^{-1} \geq B^{-1}10^{\frac{\mu_{th}+PL_{d_0}+10n\log_{10}\left(\frac{d}{d_0}\right)+P_N}{10}} = \theta_{th} \qquad (11)$$

Then, a new intermediate variable is defined as $\xi_i = \frac{1}{(1+\alpha)P_{tx,i}+P_{ct,i}}$ to transform the constraint (9c). The optimization problem **P1** is finally transformed to the form of the Geometric Program (GP), as shown in follows,

$$\textbf{P2:} \quad \max_{(\xi_i,v_i)} \sum_{i=1}^{i\in\mathcal{N}} v_i, \qquad (12a)$$

$$s.t. \quad 0 \leq \frac{v_i}{1-PLR_{i,th}}, \qquad (12b)$$

$$\frac{v_i \cdot \xi_i^{-1}}{1-PLR_{i,th}} \leq \mu_{on} \cdot R \cdot \overline{EH_i}, \qquad (12c)$$

$$\xi_i \leq \frac{1}{P_{ct,i}+(1+\alpha)\cdot\theta_{th}\cdot R}, \qquad (12d)$$

$$\frac{1}{(1+\alpha)\cdot P_{tx,\max}+P_{ct,i}} \leq \xi_i, \qquad (12e)$$

$$\xi_i \leq \frac{1}{(1+\alpha)\cdot P_{tx,\min}+P_{ct,i}}, \qquad (12f)$$

Finally, the throughput maximization problem **P2** as a classical GP can be solved efficiently by many custom solvers. Then, the optimal transmission power $P_{tx,i}^*, i \in \mathcal{C}_{node}$ and the corresponding achievable throughput $v_i^*, i \in \mathcal{C}_{node}$ can be obtained.

C. Source Rate Configuration

Once, the optimal throughput for each node is obtained through solving the throughput maximization problem with the time-varying different EH states. Then, the source rates for each node can be configured according to the optimal achievable throughput. In addition, different applications have different requirements of the source rates for satisfying the effective diagnosis. For vital signals, the larger source rate means more useful information can be used for diagnosis, meanwhile the larger source rate will cost more energy to be transmitted. However, the limited energy and dynamic link quality will result in many packet losses with an exorbitant source rate, and the random packet losses will break the integrity of data. Therefore, the source rate usually has a most appropriate upper boundary S_{up} of the source rate, which contains enough information for diagnosis. In addition, the source rate also have a acceptable low boundary S_{low}. When the source rate is lower than the low boundary S_{low}, the vital data will lose the diagnostic significance. Therefore, the boundaries of the source rate as well as the optimal achievable throughput jointly determine the configuration value of the source rate as follows,

$$S_i = \max\{\min(v_i^*, S_{up,i}), S_{low,i}\} \qquad (13)$$

When the optimal achievable throughput v^* is larger than the upper boundary S_{up}, it means the harvesting energy by the harvester is enough for supporting the source rate S_{up}, meanwhile the long-term PLR performance is also satisfied by solving the maximization problem **P2**. Then, the source rate is set to the upper boundary S_{up} for the best diagnosis. When the throughput v^* is in the range of $[S_{low}, S_{up}]$, the source rate is set to the optimal throughput v^* to just meet the throughput requirements for keeping more details of the data signals. Otherwise, the source rate is configured as the low boundary S_{low} to ensure the diagnostic significance. However, the throughput condition cannot be satisfied with current energy harvesting rate, and there will be packets blocked in the data queue. In the following section, we design the short-term QoS aware resource allocation scheme to solve the problem.

IV. SHORT-TERM QoS AWARE SLOT ALLOCATION SCHEME

In the above section, the long-term QoS performance is considered with the time-varying EH states from statistical analysis. However, the time-varying EH states and dynamic link quality may cause the fluctuations of the data queue. In this section, we explore the time slot allocation to further improve the short-term QoS performance. Firstly, we analyze the energy harvesting process in details. Then, the sensor state evaluation method is given. Finally, the different slot allocation schemes are adopted for nodes with different states.

A. Energy Harvesting Process Analysis

For better allocating slots for each node, the time-varying and heterogeneous EH states for each node should be carefully studied to adjust the allocation of slots. As we adopt the scheduled access mechanism in beacon mode with superframe boundaries, nodes only turn active in its dedicated slots to transmit the data packets while keep sleep for saving energy in other slots. Considering the time-varying EH state, the

EH states of each node in a superframe are different, which determine how much energy the body nodes can collect for transmitting data packets. For instance, if the EH state of one node has a high probability to keep the OFF state at the beginning of the following superframe, it means the slots at the end of the following superframe can be allocated to the node for collecting more energy with more harvesting time. In this paper, only the EH states of nodes in the allocated slots of last superframe can be known by the hub, thus the EH states of each sensor in the following superframe need to be predicted for better allocating slots.

The energy harvesting process is modeled as a two-state Markov chain as shown in Fig. 1. The transition matrix can be expressed as follows,

$$\mathbf{P} = \begin{bmatrix} 1 - p_{01} & p_{01} \\ p_{10} & 1 - p_{10} \end{bmatrix} \qquad (14)$$

We define the probability of EH state to be the ON state in a x-th slot is denoted by $p(x)$, then after τ slots, the EH state has been transferred $\lceil \frac{\tau}{k} \rceil$ times. $\lceil \cdot \rceil$ is the ceiling function. Thus, the probability of the ON state after τ slots can be calculated as follows [43],

$$
\begin{aligned}
p(x + \tau) &= \begin{bmatrix} 1 - p(k) & p(k) \end{bmatrix} \cdot \mathbf{P}^{\lceil \frac{\tau}{k} \rceil} \cdot \begin{bmatrix} 0 \\ 1 \end{bmatrix} \\
&= \frac{p_{01}}{Q} + \frac{p(k) \cdot p_{10} - (1 - p(k)) \cdot p_{01}}{Q} \cdot (1 - Q)^{\lceil \frac{\tau}{k} \rceil}
\end{aligned}
\qquad (15)
$$

where $Q = p_{01} + p_{10}$. Suppose the EH state in the x-th slot is known, then the probability of the ON state $p(x)$ is equal to 0 when the EH state is OFF. Otherwise $p(x)$ is set to 1 with the ON state. Thus, the Eq. (15) can be expressed as,

$$
p(x + \tau) = \begin{cases} \frac{p_{01}}{Q} - \frac{p_{01} \cdot (1 - Q)^{\lceil \frac{\tau}{k} \rceil}}{Q}, & p(x) = 0 \\ \frac{p_{01}}{Q} + \frac{p_{10} \cdot (1 - Q)^{\lceil \frac{\tau}{k} \rceil}}{Q}, & p(x) = 1 \end{cases}
\qquad (16)
$$

Thus, the EH states of each node in the following superframe can be predicted, while the last EH state in the allocated slot of the last superframe can be obtained through the feedback from the node.

B. Sensor State Evaluation

Considering the heterogeneous EH states, the residual energy from energy harvesters is different in different nodes. For the energy-sufficient nodes, the residual energy in these nodes is enough to transmit the arriving data in the following superframe. Thus these energy-sufficient nodes are insensitive to the location of allocated slots in the following superframe, while the number of allocated slots becomes important with considering both the arriving data packets and the blocked packets in the data queue. As for the energy-constrained nodes, we need to dynamically adjust the locations of allocated slots to harvest more energy to improve the short-term QoS performance. Therefore, the nodes can be classified into two categories based on the residual energy: the energy-sufficient nodes and the energy-constrained nodes.

$$\textbf{Con1:} \quad E_{res,i} \geq [(1 + \alpha) P_{tx,i} + P_{ct,i}] \cdot \frac{S_i \cdot T}{R} \qquad (17)$$

where $E_{res,i}$ denotes the residual energy in node i. When the above condition (17) is satisfied for sensor i, the node i is divided into the GOOD node set Φ_{GOOD}. Otherwise, the node i belongs to the BAD node set Φ_{BAD}.

When allocating the time slots for each node, the nodes in Φ_{BAD}, which is sensitive to the locations of allocated slots, should be firstly allocated for the time slots. Then the rest of the nodes are allocated for these nodes in Φ_{GOOD} with considering the blocked packets in the data queue.

$$
Node_i \in \begin{cases} \Phi_{GOOD}, & \text{If \textbf{Con1} is satisfied.} \\ \Phi_{BAD}, & \text{Otherwise} \end{cases}, \forall i \in \mathcal{C}_{node} \qquad (18)
$$

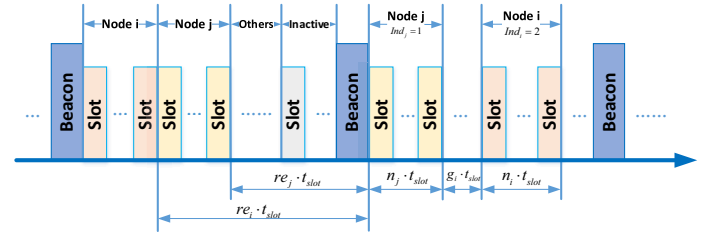### C. Slot Allocation Scheme for Energy-Constrained Nodes

Fig. 2: Details of slot allocations for each sensor.

For the energy-constrained nodes in the BAD set Φ_{BAD}, the residual energy is limited to transmit the arriving data in the next framework. Thus, it should harvest more energy before its dedicated slot in the following framework. Generally, the node with the allocated slot at the end of the superframe will have more time to collect energy. Due to the time-varying and heterogeneous EH states for nodes, there may be several nodes in the BAD set Φ_{BAD}, thus we should dynamic allocate the slots for each node with considering both the number and the locations.

Firstly, we evaluate how long each sensor will take to harvest enough energy to transmit the arriving data. The probability of the ON state in the last allocated slot can be obtained by the hub through the feedback from the node i, which is regard as $p_i(0)$. In addition, the probability of the ON state for the following slots can be predicted as the equation (16). Thus, the total harvesting energy after m slots on average from the last allocated slot is calculated as follows,

$$F_{i,EH}(m) = \sum_{l=1}^{m} \left(p_i (re_i + l) \cdot \overline{EH_i} \cdot t_{slot} \right) \qquad (19)$$

where re_i is the number of slots from the last allocated slot to the current beacon as shown in Fig. 2. Obviously, the function $F_{i,EH}(m)$ is a monotone function of time. Therefore, we can obtain the needed number of slots after the current beacon, called the expected waiting time η_i for node i, to harvest enough energy to transmit the arriving data as the following equation,

$$\eta_i = \arg_m \left\{ F_{i,EH}(m) = [(1 + \alpha) P_{tx,i} + P_{ct,i}] \cdot \frac{S_i \cdot T}{R} \right\} \qquad (20)$$

For different nodes in Φ_{BAD}, the node with the larger expected waiting time η means that it needs more time to harvest energy before the next transmissions, thus it should be

allocated the slots after the nodes with the smaller expected waiting time η. So the expected waiting time η can be used to sort the nodes for allocating slots.

After ordering the nodes, the slot allocation consists of two aspects: the number of slots and the locations of slots. As shown in Fig. 2, the specific allocated slots for sensor i can be determined by two parameters: g_i and n_i. g_i represents the number of slots between the end of allocated slots for previous node and the begin of allocated slots for node i, while n_i denotes the number of allocated slots for node i. Finally, the slot allocation problem can be state as: to maximize the difference between the location and the expected waiting time of all nodes for achieving more energy for these energy-constrained nodes by optimizing the number and the locations of slots for each sensor. Mathematically, the problem can be formulated as follows,

$$\textbf{P3:} \quad \max_{(g_i, n_i)} G_{sum}(\eta_i, g_i, n_i), \tag{21a}$$

$$s.t. \quad \sum_{i \in \Phi_{BAD}} (g_i + n_i) \leq M, \tag{21b}$$

$$R \cdot n_i \cdot t_{slot} \geq D_i, \tag{21c}$$

$$g_i, n_i \in \mathbb{N}, i \in \Phi_{BAD}, \tag{21d}$$

where G_{sum} is the sum distance between the location and the expected waiting time of all nodes as the objective function, which can be expressed as follows,

$$G_{sum}(\eta_i, g_i, n_i) = \sum_{i \in \Phi_{BAD}} \left(\sum_{\{j \in \Phi_{BAD} | \eta_j < \eta_i\}} (g_j + n_j) + g_i - \eta_i \right). \tag{22}$$

In the constraint (21b), the number of allocated slots should be less than the total number M of slots in a superframe. As for the constraint (21c), the number of allocated slots for each sensor should be able to transmit the arriving data with considering the packet loss rate, where the equivalent arriving data D_i for node i can be expressed as follows,

$$D_i = \frac{S_i \cdot \left(re_i + \sum_{\{j \in \Phi_{BAD} | \eta_j \leq \eta_i\}} (g_j + n_j) \right) \cdot t_{slot}}{(1 - PLR_{i,th})} \tag{23}$$

The slot allocation problem **P3** is an Integer Linear Programming (ILP), which can be solved efficiently [42]. After allocating slots for the energy-constrained nodes, the remaining slots are then assigned to the energy-sufficient nodes in the GOOD set Φ_{GOOD}.

D. Slot Allocation Scheme for Energy-Sufficient Nodes

Compared with the energy-constrained nodes, the energy-sufficient nodes have enough energy to transmit the arriving data, and they are insensitive to the locations of allocated slots. Considering the time-varying EH states, some data packets may be blocked in the data queue with the dynamic link quality. If the blocked data packets cannot be transmitted to the hub, they will lead to the increasing delay of not only the blocked packets but also the arriving packets [32]. Therefore, the blocked data packets in the data queue need to

be transmitted for improving the short-term QoS performance, when there are sufficient residual energy in the energy buffer.

Considering both the blocked data D_{block} in the data queue and the arriving data in the following superframe, the total data D_{buf} can be expressed as follows,

$$D_{buf,i} = D_{block,i} + S_i \cdot T \tag{24}$$

The remaining number of slots N_{rest} after the slot allocation for energy-constrained nodes can be calculated as follows,

$$N_{rest} = M - \sum_{i \in \Phi_{BAD}} n_i \tag{25}$$

Thus, the total number of the allocated slots for the energy-sufficient nodes should be not larger than the remaining number of slots N_{rest}, given as follows,

$$\sum_{i \in \Phi_{GOOD}} n_i \leq N_{rest} \tag{26}$$

For different energy-sufficient nodes, they expect to be allocated enough slots for transmitting both the blocked data and the arriving data. However, there should be enough energy for supporting the transmission in the energy buffer, as satisfying the following constraints,

$$E_{res,i} + \overline{EH_i} \cdot T \geq [(1 + \alpha) P_{tx,i} + P_{ct,i}] \cdot n_i \cdot t_{slot} \tag{27}$$

To evaluate the satisfaction of both the blocked data and the arriving data with given number of slots, a utility function $U(m, D_{buf})$ is defined as follows,

$$U(m, D_{buf}) = \frac{((R \cdot m \cdot t_{slot})^2 - 2 \cdot (R \cdot m \cdot t_{slot}) \cdot D_{buf})}{D_{buf}^2} \tag{28}$$

When the number of allocated slots is less than $\frac{D_{buf}}{R \cdot t_{slot}}$, more allocated slots can achieve a higher utility to transmit more data in the queue buffer. When the number of the allocated slots reaches the value $\frac{D_{buf}}{R \cdot t_{slot}}$, the node obtain the highest utility. If still increasing the number of allocated slots, it will cause the waste of the channel resources, thus the utility will decrease correspondingly. Finally, the slot allocation problem for the energy-sufficient nodes can be formulated to maximize the total utility of all nodes in GOOD set, subject to the total slot constraint and the energy constraint. Mathematically, the slot optimization problem can be written as follows,

$$\textbf{P4:} \quad \max_{(n_i)} \sum_{i \in \Phi_{GOOD}} U(n_i, D_{buf,i}), \tag{29a}$$

$$s.t. \quad \sum_{i \in \Phi_{GOOD}} n_i \leq N_{rest}, \tag{29b}$$

$$E_{res,i} + \overline{EH_i} \cdot T \geq [(1 + \alpha) P_{tx,i} + P_{ct,i}] \cdot n_i \cdot t_{slot}, \tag{29c}$$

$$n_i \in \mathbb{N}, i \in \Phi_{GOOD}, \tag{29d}$$

With respect to **P4**, the problem is a classical Quadratic Problem (QP), which can also be solve efficiently with using many custom solvers [44].

TABLE I: Parameters of body nodes for different postures

Index	d	n	PL_{d_0}	$\sigma_S (dB)$			Data Rate	
				Still	Walk	Run	S_{up}	S_{low}
1	69	3.11	35.2	6.1	5.4	5.7	40	20
2	36	3.23	41.2	4.8	7.4	7.8	68	30
3	48	3.35	32.2	5.1	4.9	4.5	34	16
4	34	3.45	32.5	2.6	4.4	4.0	50	25
5	100	3.11	35.2	2.2	3.6	2.6	35	16

V. Simulation results

In this section, we investigate the performance of the proposed Power-Rate-Slot resource allocation scheme in terms of average PLR, packet delay, throughput and energy efficiency. To evaluate the effectiveness of the proposed algorithms, there are three comparison schemes: the offline scheme [26], the online scheme [6] and the fixed scheme. Due to the lack of the IEEE 802.15.6-based hardware, we develop an event-driven WBAN system in the MATLAB. An MATLAB-based optimization toolbox, YALMIP [44], is embedded in the simulation environment to solve the proposed optimization problems. To better simulate the channel, the channel reference code by IEEE 802.15.6 standard [45] is adopted as the channel module in the WBAN system.

A. Simulation Setup

Above all, the WBAN simulation settings should be illustrated in details. We consider a classical WBAN system, which contains one hub and five $N = 5$ wireless body nodes. The deployed positions and link parameters of all nodes are given in Table I, referring to the actual link experiment results in [40] [39]. The changes of postures are modeled as a Markov chain, and we only consider three most common postures, i.e., still, walk and run with 0.5, 0.3 and 0.2 steady-state probabilities, correspondingly. Besides, we assume the hub can identify the changes of postures with high accuracy in real-time [46]. The extension to more body postures is straightforward. The standard derivation σ_s of the shadowing changes with the postures, while the mean of the shadowing can be used to indicate the quality of the environment [40]. In this paper, we assume the hub has sufficient energy supply, while the body nodes are powered by a piezoelectric energy harvester according to the intensity of body movements. Considering the different intensity of body parts, the energy harvesting rates of different body nodes are heterogeneous, which also change with the postures, as well as the steady state probabilities of the EH states [6], as shown in Table II. Other parameters are selected according to the IEEE 802.15.6 specifications [31].

B. The Effectiveness of Long-term Power-Rate Control Scheme

Firstly, we analyze the allocated results of the long-term power-rate control scheme (PRCS) for different postures. As shown in Table I, the parameters of the path loss are different to different nodes as well as the source rate, meanwhile the statistical characterizations of the shadowing fluctuate for different postures. Thus, the resource allocation schemes should be able to deal with the dynamic link quality. The

allocated transmission power and configured source rates for different nodes by the proposed PRCS in different postures are given in Figure 3. In the PRCS, we optimize the transmission power for each node based on the link quality to support the long-term QoS performance. Thus, the allocated transmission powers for each node are dynamically adjusted when the link quality changes due to the postures in Figure 3(a). For instance, the node 3 and the node 4 are close to the hub, and their link qualities are much better than the other nodes. Hence, the transmission powers for them are assigned a lower value to save precious energy under the condition of satisfying the long-term QoS requirements.

In addition, the source rates for different nodes are configured based on the heterogeneous requirements and the energy harvesting rates. As shown in Figure 3(b), the source rates of the node 1 and the node 2 are configured as the low boundary S_{low} in all postures. This is because the highest energy harvesting rates of them are still not enough for supporting the optimal source rate S_{up} with the higher transmission power in Figure 3(a). As for node 5, the energy harvesting rates in different postures are different for the piezoelectric energy harvester in Table II. Thus, the source rates are configured, correspondingly.
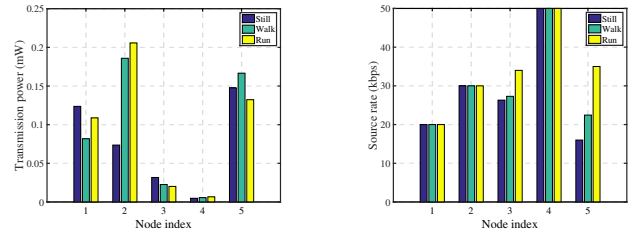
(a) Allocated transmission power by PRCS

(b) Configured source rate by PRCS

Fig. 3: Allocated results for different nodes in different postures by the proposed PRCS.

C. The Effectiveness of Short-term QoS Aware Slot Allocation Scheme

Secondly, we evaluate the effectiveness of the short-term QoS aware slot allocation scheme (QASAS). Considering the dynamic link qualities, the packet losses will occur with uncertainty. Besides, the arriving energy in a superframe is also time-varying, thus the number of the blocked packets cannot be predicted. If the blocked packets cannot be transmitted to the hub, not only the blocked packets but also the arriving packets will have a high packet delay, and even it will cause the packet losses due to the packet delay over the preset threshold or the packet buffer overflow.

Compared with the long-term PRCS, the short-term QASAS can give a timely response to the changes of the packet buffer state and the energy buffer state. When there are many blocked packets in the packet buffer and residual energy in the energy buffer, more slots will be allocated for transmitting the blocked packets based on the level of the residual energy. As shown in Figure 4(a), the number of packets keeps at a high level without using the QASAS. Fortunately, the QASAS can timely

TABLE II: Parameters of energy harvesters

Node index	Still (mW)			Walk (mW)			Run (mW)		
	EH_{min}	EH_{max}	μ_{on}	EH_{min}	EH_{max}	μ_{on}	EH_{min}	EH_{max}	μ_{on}
1	0.01	0.015	0.9	0.04	0.05	0.3	0.06	0.07	0.4
2	0.02	0.025	0.8	0.06	0.07	0.4	0.09	0.11	0.5
3	0.015	0.02	0.9	0.035	0.05	0.3	0.04	0.06	0.45
4	0.03	0.04	0.8	0.055	0.06	0.4	0.07	0.08	0.6
5	0.02	0.03	0.7	0.08	0.10	0.6	0.09	0.11	0.8

TABLE III: EH-powered WBAN simulation parameters

Parameter	Description	Value
B	bandwidth	1MHz
P_N	noise power	-94dBm
α	power amplifier inefficiency	2.4
E_{ct}	circuitry energy consumption	50uW
t_{slot}	time length of one time slot	0.5ms
R	transmission rate	485.6kbps
$P_{tx,min}$	minimum value of the transmission power	-30dBm
$P_{tx,max}$	maximum value of the transmission power	0dBm
PLR_{th}	preset threshold of the packet loss rate	5%
$Delay_{th}$	preset threshold of the packet delay	500ms
D_{buf}	packet buffer size	100kb

transmit the blocked packets based on the packet buffer state and the energy buffer state, hence, the number of the packet buffer can stay a low level as shown in Figure 4(b).
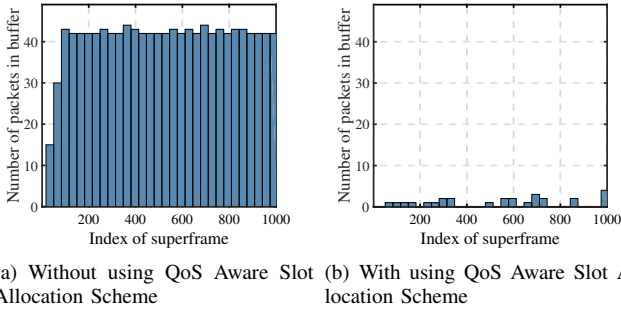

(a) Without using QoS Aware Slot Allocation Scheme (b) With using QoS Aware Slot Allocation Scheme

Fig. 4: Number of packets in the buffer of node 4 changes before and after adopting the QoS Aware Slot Allocation Scheme (QASAS).

D. The Influence of Different Mean of Shadowing on Performance

For evaluating the effectiveness of the long-term power-rate control scheme and the short-term slot allocation scheme, we compare them with three comparison schemes: the offline scheme [26], the online scheme [6] and the fixed scheme in terms of the average PLR, packet delay, throughput and energy per bit. For simulating the impact of the changes in the environment on the QoS performance, the mean of the shadowing can be adjusted to change the statistical characterization of the wireless channel. The higher mean of the shadowing represents the worse link quality of the wireless channel. In this paper, we assume all nodes have the same mean of the shadowing for the sake of simplification, and study the influence of the mean of the shadowing on the QoS performance.

As shown in Figure 5(a) and Figure 5(b), the proposed PRS-RA scheme obtains the lowest PLR performance and the lowest packet delay which satisfying the QoS requirements, even comparing with the offline scheme. This is because the proposed PRS-RA scheme considers both the long-term QoS performance and the short-term QoS performance though the adaption of the source rate, the transmission power and the slots. However, due to the priori knowledge of the channel state and EH states, the offline scheme can optimally allocated the transmission power to maximize the throughput as shown in Figure 5(d). In addition, the transmission power is adjusted in real-time based on the real-time path loss of the channel, thus the energy efficiency is the highest as shown in Figure 5(c). Meanwhile, both the proposed PRS-RA scheme and online scheme assume that only the statistical information of channel state and the EH states are priori known by the hub. However, the proposed PRS-RA scheme has a higher energy efficiency performance than the online scheme, which is very close to the offline scheme. This is because the optimal transmission power is firstly allocated to support the long-term QoS performance, and then the effective slot allocation can further guarantee there is enough power to transmit the data packets in the allocated slots, which can avoid the waste of energy due to the packet losses.

As for the throughput in Figure 5(d), the throughput of the proposed PRS-RA scheme decreases with the mean of the shadowing, while the energy cost per bit increases with the mean of the shadowing in Figure 5(c). When the link quality becomes worse with a higher mean of the shadowing, the long-term power-rate control scheme (PRCS) dynamically adjust the transmission rate and the source rate based on the link quality. Generally, the transmission power will be increased to guarantee the QoS performance and the source rate will be decreased to ensure the integrity of data with a lower PLR. In addition, the short-term QoS aware slot allocation scheme (QASAS) dynamically analyzes the state of each node, and then optimizes the appropriate slots to cope with the blocked packets in the buffer. Hence, the bandwidth utilization of the proposed PRA-SA reaches to 94%, which is higher than the online scheme, thus, more channel resource can be utilized by other WBANs.

E. The Influence of Different EH Efficiencies on Performance

To evaluate the effectiveness of the long-term power-rate control scheme (PRCS) and the short-term QoS aware slot allocation scheme (QASAS), we compare three different schemes: 1) the proposed PRS-RA with both PRCS and QASAS, 2) the proposed PRS-RA only with PRCS, 3) the proposed PRS-RA only with QASAS. And we gradually
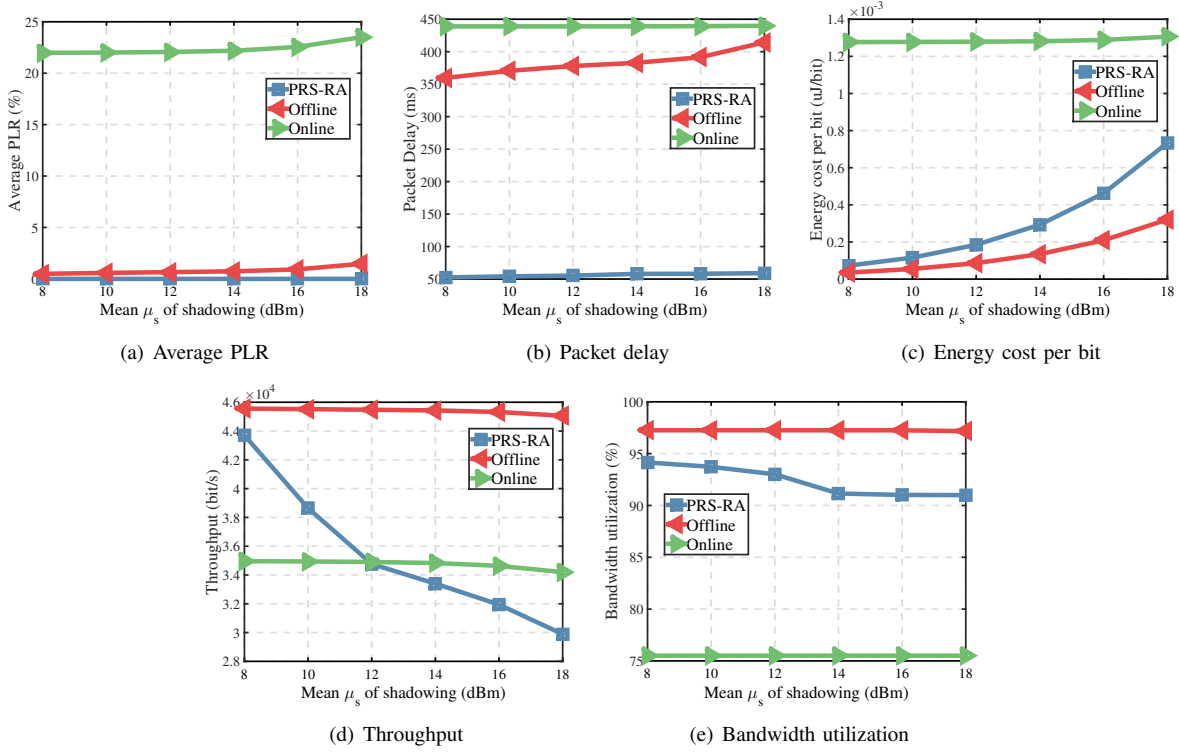
Fig. 5: The QoS performance of different algorithms.

(a) Average PLR performance

(b) Packet delay performance

(c) Throughput performance

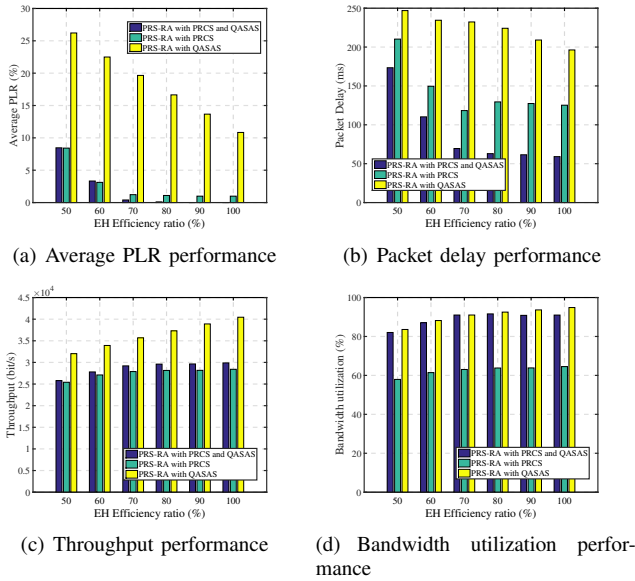(d) Bandwidth utilization performance

Fig. 6: QoS performances versus the EH efficiency ratio.

change EH efficiency ratio for all nodes to scale the range of the energy harvesting rate $[EH_{min}, EH_{max}]$. The smaller EH efficiency ratio means energy harvester can collect less energy when the energy harvester stays the ON state. The QoS performances versus the EH efficiency ratio are given in Figure 6.

The nodes can collect more energy with a higher EH efficiency ratio, thus the average PLRs of all three schemes

decrease with the EH efficiency ratio as shown in Figure 6(a). And the PRS-RA with both PRCS and QASAS outperform the other schemes, and it can achieve almost 0% PLR performance. In addition, the PRS-RA with only PRCS has a lower PLR than the PRS-RA with only QASAS, this is because the optimization allocation of the transmission power and the source rate can support the long-term QoS performance, while the PRS-RA with only QASAS can adjust the number of slots for each node, which cannot deal with the packet losses due to the dynamic links with a fixed transmission power. However, when the short-term QASAS combines with the long-term PRCS, not only the PLR but also the packet delay can achieve the best performance. Though the PRS-RA with only QASAS can have a highest throughput in Figure 6(c) and a highest bandwidth utilization in Figure 6(d), the highest PLR in Figure 6(a) will cost a lot of energy cost, which cannot be acceptable especially for the EH-powered WBAN system.

VI. CONCLUSION

In this paper, we optimize the resource allocations to improve both the long-term QoS and the short-term QoS performance in the EH-powered WBAN system, while the time-varying and heterogeneous EH states are fully taken into consideration. Firstly, we design a joint Power-Rate control scheme (PRCS) in terms of the transmission power and the source rate to ensure the long-term QoS performance based on both the EH states and the dynamic link quality. Secondly, we evaluate the node state in real time based on the packet buffer state and the energy buffer state, and then a QoS aware slot allocation scheme is adopted to dynamically allocate the slots

based on the node states for timely transmitting the blocked packets in the buffer. The simulation results demonstrate that the joint Power-Rate control scheme (QASAS) can effectively improve the QoS performances in terms of PLR, delay and throughput. In addition, the short-term QoS aware slot allocation scheme can timely allocate slots to transmit the blocked packets, thus the QoS performance is further improved with adopting both PRCS and QASAS.

Acknowledgment

References

[1] M. Salayma, A. Al-Dubai, I. Romdhani, and Y. Nasser, "Wireless body area network (wban): A survey on reliability, fault tolerance, and technologies coexistence," *ACM Computing Surveys (CSUR)*, vol. 50, no. 1, p. 3, 2017.

[2] S. Movassaghi, M. Abolhasan, J. Lipman, D. Smith, and A. Jamalipour, "Wireless body area networks: A survey," *IEEE Communications Surveys & Tutorials*, vol. 16, no. 3, pp. 1658–1686, 2014.

[3] C. Dagdeviren, Z. Li, and Z. L. Wang, "Energy harvesting from the animal/human body for self-powered electronics," *Annual Review of Biomedical Engineering*, vol. 19, no. 1, 2017.

[4] R. Zhang, H. Moungla, J. Yu, and A. Mehaoua, "Medium access for concurrent traffic in wireless body area networks: Protocol design and analysis," *IEEE Transactions on Vehicular Technology*, vol. 66, no. 3, pp. 2586–2599, 2017.

[5] M. Razzaque, M. T. Hira, and M. Dira, "Qos in body area networks: A survey," *ACM Transactions on Sensor Networks (TOSN)*, vol. 13, no. 3, p. 25, 2017.

[6] E. Ibarra, A. Antonopoulos, E. Kartsakli, J. J. Rodrigues, and C. Verikoukis, "Qos-aware energy management in body sensor nodes powered by human energy harvesting," *IEEE Sensors Journal*, vol. 16, no. 2, pp. 542–549, 2016.

[7] Y. Luo, P. Hong, R. Su, and K. Xue, "Resource allocation for energy harvesting-powered d2d communication underlaying cellular networks," *IEEE Transactions on Vehicular Technology*, 2017.

[8] W. Zang, S. Zhang, and Y. Li, "An accelerometer-assisted transmission power control solution for energy-efficient communications in wban," *IEEE Journal on Selected Areas in Communications*, vol. 34, no. 12, pp. 3427–3437, 2016.

[9] Z. Liu, B. Liu, and C. W. Chen, "Transmission-rate-adaption assisted energy-efficient resource allocation with qos support in wbans," *IEEE Sensors Journal*, vol. 17, no. 17, pp. 5767–5780, 2017.

[10] Y. Hao, L. Peng, H. Lu, M. M. Hassan, and A. Alamri, "Energy harvesting based body area networks for smart health," *Sensors*, vol. 17, no. 7, p. 1602, 2017.

[11] F. Akhtar and M. H. Rehmani, "Energy harvesting for self-sustainable wireless body area networks," *IT Professional*, vol. 19, no. 2, pp. 32–40, 2017.

[12] A. Kansal, J. Hsu, S. Zahedi, and M. B. Srivastava, "Power management in energy harvesting sensor networks," *ACM Transactions on Embedded Computing Systems (TECS)*, vol. 6, no. 4, p. 32, 2007.

[13] O. Ozel, K. Tutuncuoglu, J. Yang, S. Ulukus, and A. Yener, "Transmission with energy harvesting nodes in fading wireless channels: Optimal policies," *IEEE Journal on Selected Areas in Communications*, vol. 29, no. 8, pp. 1732–1743, 2011.

[14] S. Leng and A. Yener, "Resource allocation in body area networks for energy harvesting healthcare monitoring," in *Handbook of Large-Scale Distributed Computing in Smart Healthcare*, pp. 553–587, Springer, 2017.

[15] M. Wahbah, M. Alhawari, B. Mohammad, H. Saleh, and M. Ismail, "Characterization of human body-based thermal and vibration energy harvesting for wearable devices," *IEEE Journal on emerging and selected topics in circuits and systems*, vol. 4, no. 3, pp. 354–363, 2014.

[16] L. Xia, J. Cheng, N. E. Glover, and P. Chiang, "0.56 v,–20 dbm rf-powered, multi-node wireless body area network system-on-a-chip with harvesting-efficiency tracking loop," *IEEE Journal of Solid-State Circuits*, vol. 49, no. 6, pp. 1345–1355, 2014.

[17] D. El-Damak and A. P. Chandrakasan, "A 10 nw–1 μw power management ic with integrated battery management and self-startup for energy harvesting applications," *IEEE Journal of Solid-State Circuits*, vol. 51, no. 4, pp. 943–954, 2016.

[18] S. Bluetooth, "Bluetooth core specification version 4.0," *Specification of the Bluetooth System*, 2010.

[19] M. Kramer and A. Geraldy, "Energy measurements for micaz node," *University of Kaiserslautern, Kaiserslautern, Germany, Technical Report KrGe06*, 2006.

[20] A. C. W. Wong, M. Dawkins, G. Devita, N. Kasparidis, A. Katsiamis, O. King, F. Lauria, J. Schiff, and A. J. Burdett, "A 1 v 5 ma multimode ieee 802.15. 6/bluetooth low-energy wban transceiver for biotelemetry applications," *IEEE Journal of Solid-State Circuits*, vol. 48, no. 1, pp. 186–198, 2013.

[21] H. Mosavat-Jahromi, B. Maham, and T. A. Tsiftsis, "Maximizing spectral efficiency for energy harvesting-aware wban," *IEEE journal of biomedical and health informatics*, vol. 21, no. 3, pp. 732–742, 2017.

[22] B. Varan and A. Yener, "Delay constrained energy harvesting networks with limited energy and data storage," *IEEE Journal on Selected Areas in Communications*, vol. 34, no. 5, pp. 1550–1564, 2016.

[23] F. Shan, J. Luo, W. Wu, M. Li, and X. Shen, "Discrete rate scheduling for packets with individual deadlines in energy harvesting systems," *IEEE Journal on Selected Areas in Communications*, vol. 33, no. 3, pp. 438–451, 2015.

[24] K. Tutuncuoglu and A. Yener, "Optimum transmission policies for battery limited energy harvesting nodes," *IEEE Transactions on Wireless Communications*, vol. 11, no. 3, pp. 1180–1189, 2012.

[25] S. Wei, W. Guan, and K. R. Liu, "Power scheduling for energy harvesting wireless communications with battery capacity constraint," *IEEE Transactions on Wireless Communications*, vol. 14, no. 8, pp. 4640–4653, 2015.

[26] C. Huang, R. Zhang, and S. Cui, "Optimal power allocation for outage probability minimization in fading channels with energy harvesting constraints," *IEEE Transactions on Wireless Communications*, vol. 13, no. 2, pp. 1074–1087, 2014.

[27] M. Alhawari, T. Tekeste, B. Mohammad, H. Saleh, and M. Ismail, "Power management unit for multi-source energy harvesting in wearable electronics," in *Circuits and Systems (MWSCAS), 2016 IEEE 59th International Midwest Symposium on*, pp. 1–4, IEEE, 2016.

[28] A. Dionisi, D. Marioli, E. Sardini, and M. Serpelloni, "Autonomous wearable system for vital signs measurement with energy-harvesting module," *IEEE Transactions on Instrumentation and Measurement*, vol. 65, no. 6, pp. 1423–1434, 2016.

[29] D. Shaviv and A. Özgür, "Universally near optimal online power control for energy harvesting nodes," *IEEE Journal on Selected Areas in Communications*, vol. 34, no. 12, pp. 3620–3631, 2016.

[30] B. Liu, S. Yu, and C. W. Chenz, "Optimal resource allocation in energy harvesting-powered body sensor networks," in *Future Information and Communication Technologies for Ubiquitous HealthCare (Ubi-HealthTech), 2015 2nd International Symposium on*, pp. 1–5, IEEE, 2015.

[31] I. S. Association *et al.*, "Ieee standard for local and metropolitan area networks part 15.6: Wireless body area networks," *IEEE Standard for Information Technology, IEEE*, vol. 802, no. 6, pp. 1–271, 2012.

[32] Z. Liu, B. Liu, and C. W. Chen, "Buffer-aware resource allocation scheme with energy efficiency and qos effectiveness in wireless body area networks," *IEEE Access*, vol. 5, pp. 20763–20776, 2017.

[33] M. Geisler, S. Boisseau, M. Perez, P. Gasnier, J. Willemin, I. Ait-Ali, and S. Perraud, "Human-motion energy harvester for autonomous body area sensors," *Smart Materials and Structures*, vol. 26, no. 3, p. 035028, 2017.

[34] M. Thielen, L. Sigrist, M. Magno, C. Hierold, and L. Benini, "Human body heat for powering wearable devices: From thermal energy to application," *Energy Conversion and Management*, vol. 131, pp. 44–54, 2017.

[35] A. Seyedi and B. Sikdar, "Energy efficient transmission strategies for body sensor networks with energy harvesting," *IEEE Transactions on Communications*, vol. 58, no. 7, pp. 2116–2126, 2010.

[36] S. Xiao, A. Dhamdhere, V. Sivaraman, and A. Burdett, "Transmission power control in body area sensor networks for healthcare monitoring," *IEEE Journal on Selected Areas in Communications*, vol. 27, no. 1, pp. 37–48, 2009.

[37] Y. He, W. Zhu, and L. Guan, "Optimal resource allocation for pervasive health monitoring systems with body sensor networks," *IEEE Transactions on Mobile Computing*, vol. 10, no. 11, pp. 1558–1575, 2011.

[38] L. Lin, K.-J. Wong, S.-L. Tan, and S.-J. Phee, "Asymmetric multihop networks for multi-capsule communications within the gastrointestinal tract," in *Wearable and Implantable Body Sensor Networks, 2009. BSN 2009. Sixth International Workshop on*, pp. 82–86, IEEE, 2009.

[39] E. Reusens, W. Joseph, B. Latré, B. Braem, G. Vermeeren, E. Tanghe, L. Martens, I. Moerman, and C. Blondia, "Characterization of on-body communication channel and energy efficient topology design for wireless body area networks," *IEEE Transactions on Information Technology in*

Biomedicine, vol. 13, no. 6, pp. 933–945, 2009.

[40] R. DErrico and L. Ouvry, "A statistical model for on-body dynamic channels," *International journal of wireless information networks*, vol. 17, no. 3-4, pp. 92–104, 2010.

[41] A. Goldsmith, *Wireless communications*. Cambridge university press, 2005.

[42] S. Boyd and L. Vandenberghe, *Convex optimization*. Cambridge university press, 2004.

[43] Y. Tselishchev, L. Libman, and A. Boulis, "Reducing transmission losses in body area networks using variable tdma scheduling," in *World of Wireless, Mobile and Multimedia Networks (WoWMoM), 2011 IEEE International Symposium on a*, pp. 1–10, IEEE, 2011.

[44] J. Lofberg, "Yalmip: A toolbox for modeling and optimization in matlab," in *Computer Aided Control Systems Design, 2004 IEEE International Symposium on*, pp. 284–289, IEEE, 2004.

[45] K. Yazdandoost and K. Sayrafian, "Channel model for body area network (ban), ieee p802. 15-08-0780-09-0006," *IEEE 802.15 Working Group Document*, 2009.

[46] Q. Guo, B. Liu, and C. W. Chen, "A two-layer and multi-strategy framework for human activity recognition using smartphone," in *Communications (ICC), 2016 IEEE International Conference on*, pp. 1–6, IEEE, 2016.

Zhiqiang Liu received the B.S degrees in electrical engineering from University of Science and Technology of China, Hefei, Anhui, China, in 2013, and he is currently pursuing the Ph.D. degree in electrical engineering from University of Science and Technology of China. His research interests lie resource allocation, energy-saving and Quality of Service guarantee in wireless body area networks.

Bin Liu received the B.S. and M.S. degrees, both in electrical engineering, from University of Science and Technology of China, Hefei, Anhui, China, in 1998 and 2001, respectively, and the Ph.D. degree in electrical engineering from Syracuse University, Syracuse, NY, in 2006. Currently, he is an Associate Professor with the School of Information Science and Technology, University of Science and Technology of China. His research interests are signal processing and communications in wireless sensor and body area networks.

Chang Wen Chen (F'04) is a Professor of Computer Science and Engineering at the State University of New York at Buffalo, USA. Previously, he was Allen S. Henry Endowed Chair Professor at Florida Institute of Technology from 2003 to 2007, a faculty member at the University of Missouri - Columbia from 1996 to 2003 and at the University of Rochester, Rochester, NY, from 1992 to 1996. He has been the Editor-in-Chief for IEEE Trans. Multimedia since 2014. He has also served as the Editor-in-Chief for IEEE Trans. Circuits and Systems for Video Technology from January 2006 to December 2009 and an Editor for Proceedings of IEEE, IEEE TMM, IEEE JSAC, IEEE JETCAS, and IEEE Multimedia Magazine. He and his students have received eight (8) Best Paper Awards or Best Student Paper Awards and have been placed among Best Paper Award finalists many times. He is a recipient of Sigma Xi Excellence in Graduate Research Mentoring Award in 2003, Alexander von Humboldt Research Award in 2009, and SUNY-Buffalo Exceptional Scholar - Sustained Achievements Award in 2012. He is an IEEE Fellow and an SPIE Fellow.